Chapter 14

Spectral Radiation Measurements and Analysis in the ARM Program

E. J. MLAWER

Atmospheric and Environmental Research, Lexington, Massachusetts

D. D. TURNER

National Severe Storms Laboratory, NOAA, Norman, Oklahoma

1. Introduction

The spectral signatures of radiation produced by various atmospheric constituents are key to our understanding of many issues related to climate and weather. Ground-based measurements of spectrally resolved radiation are particularly rich sources of information on atmospheric gases, clouds, and aerosol properties. For there to be confidence in simulations by atmospheric models, including general circulation models (GCMs), it is essential that calculations by the most accurate radiative transfer codes be able to reproduce these spectral measurements for a broad range of conditions. This perspective was central to the founding objectives of the ARM Program, provided an essential focus of the program during its early years, and was at the core of many of the program's important accomplishments during its history.

A critical motivation for establishing the Atmospheric Radiation Measurement (ARM) Program was to develop the capability to evaluate and improve line-by-line radiation codes, which are the most physically based radiative transfer algorithms, through extensive comparisons with high-quality spectral radiation measurements. In particular, results from the Intercomparison of Radiation Codes in Climate Models (ICRCCM; Ellingson and Fouquart 1991; Ellingson et al. 2016, chapter 1), although directed at the evaluation of the performance of fast radiation parameterizations, were key to establishing the impetus for a program such as ARM with a spectral radiation focus. A key conclusion from the analysis of longwave ICRCCM results (Ellingson et al. 1991) was that, although many fast radiation codes used within climate models had spectral errors that partially canceled out when fluxes over a wide spectral range were computed, line-by-line modelers did not have sufficient confidence in their own models to advocate using them as references. The participants in this study therefore recommended that "a program be organized to simultaneously measure the spectral radiance at high spectral resolution along with the atmospheric variables necessary to calculate the radiance, particularly for clear-sky conditions" (p. 8952). The ARM Program was developed as the answer to this challenge, and this chapter (along with other related chapters in this monograph) details the research program that was followed toward its successful resolution.

The initial response to the ICRCCM recommendation to improve radiative transfer parameterizations through the analysis of field observations was the organization of the Spectral Radiation Experiment (SPECTRE; Ellingson and Wiscombe 1996; Ellingson et al. 2016, chapter 1). This one-month field experiment deployed several infrared interferometers to Coffeyville, Kansas, to measure the downwelling infrared spectral radiance along with a range of sensors, both in situ (e.g., radiosonde, flask measurements of trace gases like carbon dioxide and methane, etc.) and remote (e.g., Raman lidar, Radio Acoustic Sounding System, cloud radar), to characterize the atmospheric state needed as input to drive the radiation models. SPECTRE, although limited, had a number of successes. The Atmospheric Emitted Radiance Interferometer (AERI; Knuteson et al. 2004a,b), which was developed by the University of Wisconsin–Madison, was demonstrated to have a robust

Corresponding author address: E. J. Mlawer, Atmospheric and Environmental Research Inc., 131 Hartwell Ave., Lexington, MA 02421.
E-mail: emlawer@aer.com

DOI: 10.1175/AMSMONOGRAPHS-D-15-0027.1

© 2016 American Meteorological Society

Brought to you by NOAA Central Library | Unauthenticated | Downloaded 07/19/23 03:21 PM UTC

calibration, and the initial comparisons showed a much better level of agreement between the observed and line-by-line calculated radiances than the range between calculations that was demonstrated during ICRCCM. The SPECTRE dataset, however, was from a single location and from a short duration campaign, a limitation that the ARM Program, which was developed based on the SPECTRE experience and science plan, was designed to overcome. A central objective of the ARM Program was to "relate observed radiative fluxes in the atmosphere, spectrally resolved and as a function of position and time, to the atmospheric temperature, composition (specifically including water vapor and clouds), and surface radiative properties" (Stokes and Schwartz 1994, p. 1203). ARM data would provide the observations at the different climatic locations over longer time periods to fulfill the critical recommendation of ICRCCM.

This chapter provides a history of some of the ARM Program's accomplishments in the analysis of spectral radiation measurements. The program has had greater successes in the thermal infrared spectral region than in the solar, primarily due to the development of the AERI in the early years of the program. [See Turner et al. (2016, chapter 13) for a short history of the development of this instrument.] Progress in the shortwave portion of the spectrum was more challenging due to the relatively few groups developing instruments to measure spectrally resolved radiance observations in that spectral region; instrumental challenges (especially for accurate radiative and spectral calibration) were more daunting than for the longwave. Much of the analysis of spectral radiation focused on clear skies in order to improve the accuracy of the emission and absorption of atmospheric gases and aerosols, with valuable results obtained from ARM spectral radiometers deployed in a number of diverse locations. As will be seen below, a recurring theme of these investigations is the nature of continuum absorption due to water vapor, an important factor in the flow of radiant energy in our atmosphere. As the program's cloud observations matured and new algorithms were developed to retrieve cloud macro- and microphysical properties (Kollias et al. 2016, chapter 17; Shupe et al. 2016, chapter 19), characterizing and improving the spectral radiative transfer algorithms in cloudy atmospheres has taken on a more prominent role. This topic is addressed in section 5 of this chapter.

2. Clear-sky longwave studies

The paradigm used in the ARM Program for analysis of spectral radiation observations is the radiative closure study, which involves the simultaneous critical evaluation of 1) the spectral radiance observations, 2) the physics and implementation of the radiative transfer model, and 3) the specification of the temperature, humidity, and other atmospheric and surface properties relevant to radiation. The evaluation includes any observations on which these properties are based and are required by the radiative transfer model. The efforts to evaluate and improve radiative transfer models in the ARM Program through this approach were undertaken and led by members of the Instantaneous Radiative Flux (IRF) working group, most notably Bob Ellingson, Tony Clough, and Hank Revercomb, within the ARM Science Team. Since the ARM data were collected routinely, the IRF developed the idea of the Quality Measurement Experiment (QME; Turner et al. 2004) to routinely perform the radiative transfer calculations and some higher-order processing needed for the radiative closure experiment.

With respect to the evaluation and improvement of line-by-line radiative transfer codes, the ARM closure studies focused mostly on the spectroscopic properties of water vapor. Although the strengths, widths, and other properties of H_2O absorption lines were scrutinized in these studies, a great deal of attention was focused on analysis related to H_2O self and foreign continuum absorption. This was anticipated in the longwave ICRCCM study, which concluded that uncertainty in the H_2O continuum led to significant limitations in climate studies (Ellingson et al. 1991). As will be seen, efforts within the ARM Program directed at attaining a comprehensive understanding of the properties of the longwave H_2O continuum ended up requiring spectrally resolved observations from several different locations. Although the program did provide some support for directed spectroscopic studies (e.g., Rothman 1992; Varanasi 1998), the primary avenue within ARM for advancement in this area relied on the analysis of field observations of spectrally resolved radiances.

a. Improvements to the modeling of water vapor absorption

The primary QME organized by the IRF compared the spectral infrared radiances observed by the AERI and computed by the line-by-line radiative transfer model (LBLRTM; Clough et al. 1992; 2005). Atmospheric state measurements were a critical component of this QME. In particular, the uncertainty in water vapor profile measurements was determined to be the limiting factor in improving the clear-sky longwave radiative transfer model (Revercomb et al. 2003). To reduce these uncertainties to a level where the water vapor profiles could be used with sufficient confidence, a concentrated effort and a series of field experiments were conducted at the ARM Southern Great Plains (SGP) and North Slope of Alaska (NSA) sites. Turner et al. (2016, chapter 13) provides a history

Brought to you by NOAA Central Library | Unauthenticated | Downloaded 07/19/23 03:21 PM UTC

of this work, without which improvements in the infrared radiation modeling would not have been possible.

The prototype AERI-00, which used liquid nitrogen to cryogenically cool its detectors and thus required manual attention to refill the liquid nitrogen dewar, was installed at the SGP site in late 1993. Even with sizable uncertainties in the H_2O profiles, the IRF anticipated similar results from AERI-LBLRTM comparisons from this deployment as were experienced during SPECTRE. However, the comparison between the AERI and LBLRTM in clear skies showed a much larger bias than was seen in SPECTRE; importantly, this large bias was seen in all seasons. The change in the size of the bias between the SPECTRE and early ARM results led to many heated discussions on the source of the bias: was it a problem with the AERI observations, aerosols that needed to be included in the calculation (perhaps the SPECTRE results were just ''lucky'' to have very low aerosol loading), or some problem with the atmospheric state (temperature and humidity) observations? This problem was not resolved until the AERI-01—the first AERI that could be run operationally by using a mechanical Sterling cooler to keep the detectors at cryogenic temperatures—was deployed to the SGP site. The side-by-side comparison of the AERI-01 and the AERI-00 showed that the bias was in the AERI-00 observations, which was traced to a small obscuration in the field of view of the AERI-00 (Knuteson et al. 1999). This served as an important lesson in deploying AERI instruments operationally, and all future AERIs (from the AERI-01 onward) were deployed differently than the AERI-00 in order to eliminate the possible obscuration bias that affected the original AERI.

While the IRF was trying to understand the bias between the AERI-00 and LBLRTM, the Pilot Radiation Observation Experiment (PROBE) was conducted in 1993 in Kavieng, Papua New Guinea. A Fourier transform infrared (FTIR) spectrometer from the National Oceanic and Atmospheric Administration (NOAA) was among the instruments deployed as part of PROBE, and initial comparisons between the FTIR and LBLRTM showed very large biases between 800 and 1000 cm^{-1} in the very moist tropical atmosphere above Kavieng. This ARM-funded analysis suggested that the absorption in version 1 of the Clough–Kneizys–Davies (CKD) H_2O continuum model[1] used within the LBLRTM was too weak, and a modified version of the continuum model (version 2.1) was created. A subsequent cruise to the western Pacific by the research ship *Discoverer* in 1996, which again included the NOAA FTIR and a newer generation AERI, confirmed the results from PROBE (Han et al. 1997). Thus, the ARM Program had made its first major advancement in our understanding of H_2O continuum absorption.

Meanwhile, the IRF continued to develop the QME at the SGP site, with comparisons between AERI-01 observations and LBLRTM calculations that were presented in a series of ARM Science Team Meeting presentations from 1994 to 1999 by Pat Brown, Tony Clough, and colleagues. A great deal of effort was focused upon the improvement of the H_2O observations; ultimately the uncertainty in the accuracy of the measurement of precipitable water vapor (PWV) at SGP would drop from order 15% in the early 1990s to 3% by the early 2000s (Turner et al. 2016, chapter 13). The extended dataset at the SGP, together with these improved PWV observations, allowed the CKD model to be further refined in the 800–1300 cm^{-1} spectral region (Turner et al. 2004), the ''atmospheric window'' so important to planetary energy balance. The SGP QME data also were extremely useful in evaluating new versions of the high-resolution transmission molecular absorption (HITRAN) absorption line database, and especially the H_2O line parameters in this database (Turner et al. 2004). The improvements that were made in the main infrared window (800–1300 cm^{-1}) from the PROBE, *Discoverer*, and SGP datasets removed a significant amount of spectral cancelation of error, and contributed significantly to the improvement of the downwelling longwave flux calculation by the LBLRTM by approximately 5 $W\,m^{-2}$ (Turner et al. 2004).

The SGP QME and tropical PROBE and *Discoverer* results were instrumental in improving the modeling of H_2O absorption, most notably H_2O continuum absorption in the atmospheric window. However, these results did not address spectroscopic issues within strong H_2O absorption bands, such as the pure rotation band from 0 to 625 cm^{-1} (>16 μm). With its participation in the Surface Heat Budget of the Arctic Ocean (SHEBA) field campaign (Uttal et al. 2002), ARM radiative closure studies were extended to these spectral regions. An extended range AERI,[2] which was modified to have sensitivity to downwelling radiation at wavenumbers as low as 400 cm^{-1} (25 μm), was deployed on the icebreaker that SHEBA used as its

[1] The water vapor continuum model used within LBLRTM during the first decade of the ARM Program was the CKD model (Clough et al. 1989), which was widely used throughout the community. In the early 2000s this model was revised and renamed the MT_CKD model (Mlawer et al. 2012). Details on these continuum formulations and their evolution over time can be found in these references; a simple explanation of the water vapor continuum is given in Turner and Mlawer (2010).

[2] The typical AERI is sensitive to radiation at wavenumbers as low as 530 cm^{-1} (19 μm).

Brought to you by NOAA Central Library | Unauthenticated | Downloaded 07/19/23 03:21 PM UTC

floating base. In the very dry Arctic atmosphere during the winter, a portion of the rotational water vapor band in the far-infrared between 100 and 625 cm^{-1} (100 to 16 μm) is partially transparent. Thus, the accuracy of the radiative transfer model can be evaluated using surface-based radiation measurements. (At larger PWV amounts, such as those seen in midlatitudes or in the tropics, this portion of the spectrum is opaque and the accuracy of the water vapor continuum or line parameters cannot be evaluated.) Tobin et al. (1999) used the AERI observations at SHEBA to demonstrate that the absorption of the CKD foreign continuum model in the far-infrared was nearly a factor of 3 too strong, leading to a significant modification to the CKD model in this spectral region.

The far-infrared accounts for nearly 40% of the total outgoing longwave radiation emitted by the planet and is very important for the radiative atmospheric heating/cooling rate profiles in the middle to upper troposphere (Clough et al. 1992; Harries et al. 2008). Thus, the improvements made by Tobin et al. (1999) had a big effect on the atmospheric heating rate profiles. However, the uncertainty in the water vapor profiles used by Tobin et al. was on the order of 25%, and this uncertainty translated directly into the same level of uncertainty in the continuum model adjustment. Furthermore, the extended-range AERI did not provide measurements in a significant portion of the far-infrared spectrum, so the accuracy of radiative transfer models in this unobserved spectral region was unable to be evaluated in SHEBA. This led ARM to organize the Radiative Heating in Underexplored Bands Campaigns (RHUBC; Turner and Mlawer 2010) to collect and analyze additional spectral radiation measurements in dry environments.

After SHEBA, the ARM Program made solid progress improving the accuracy of PWV observations in very dry climates, and by the time of the first RHUBC campaign new operational microwave radiometers at 183 GHz had been developed for deployment to the ARM NSA site (Turner et al. 2016, chapter 13). RHUBC-I deployed three of these microwave radiometers and three infrared interferometers to the NSA site in late winter 2007 to evaluate and refine the Tobin et al. modification with the improved water vapor observations. The experiment was a success. RHUBC-I demonstrated good agreement between all three of the 183-GHz radiometers, each of which used different technologies and calibration approaches (Cimini et al. 2009). Analysis of data from RHUBC-I, along with additional data collected before and after the experiment using one 183-GHz radiometer that was running operationally at NSA, demonstrated that adjustments were needed to the strengths of both the H_2O foreign and self-continuum models in the far-IR, and, importantly, refined the widths of some of the more prominent H_2O absorption lines in the 400–625 cm^{-1} region (Delamere et al. 2010).

The Delamere et al. (2010) study provided information on the strength of continuum absorption at the high wavenumber end of the H_2O pure rotation band (400–650 cm^{-1}). At the low wavenumber edge of the band (i.e., around 5 cm^{-1}), radiative closure studies at a number of microwave frequencies by Payne et al. (2011) provided analogous and consistent information on the continuum. The microwave analysis included observations at 5 cm^{-1} (150 GHz) from the deployment of the ARM Mobile Facility (AMF) to Germany in 2007 that were also analyzed by Turner et al. (2009). Based on these studies, an updated version of the continuum model (MT_CKD_2.4) was developed, with a nearly 50% change in the strength of the water vapor foreign continuum at 200 cm^{-1} (50 μm). GCM simulations demonstrated that this large change to the water vapor continuum model had a significant radiative and dynamic impact on a global climate model simulation (Turner et al. 2012a).

The success of RHUBC-I led to the second RHUBC experiment, which was conducted in fall 2009 at a high-altitude site (5.3 km AGL) in the Chilean Andes. The PWV amounts in RHUBC-II were nearly 5 times drier than the driest conditions experienced at the NSA site, and thus a larger portion of the far-infrared region was partially transparent. In particular, radiative transfer model calculations at wavenumbers as small as 220 cm^{-1} (45 μm) could be evaluated with the RHUBC-II dataset. Five interferometers were deployed during RHUBC-II, along with one of the 183-GHz radiometers from RHUBC-I. This experiment provided the first complete spectral measurement of the entire downwelling terrestrial infrared spectrum from the ground (Turner et al. 2012b) and demonstrated that to first order the current water vapor continuum model, which includes the big change at 200 cm^{-1} indicated above, is more accurate than the continuum model that existed before the RHUBC experiments.

ARM-related studies also contributed to advancements in our knowledge of the water vapor self-continuum at the short wavelength end of the AERI spectral domain. Using AERI measurements from SGP, two independent studies (Strow et al. 2006; Mlawer et al. 2012) determined that the MT_CKD self-continuum was significantly too weak from 2400 to 2600 cm^{-1}. This later study also showed that the result in this spectral region is consistent with certain laboratory and field observations of the continuum in the near-infrared.

Brought to you by NOAA Central Library | Unauthenticated | Downloaded 07/19/23 03:21 PM UTC

b. Other modeling advances in the infrared

Gaseous species other than water vapor also had their infrared spectroscopy evaluated and improved using ARM AERI observations. In 2002, AERI measurements from the NSA site were used, along with measurements from the University of Wisconsin's airborne High-resolution Interferometer Sounder (HIS) and Scanning HIS (S-HIS), to modify the carbon dioxide line shape and carbon dioxide continuum used in the 500–900 cm^{-1} region in LBLRTM. After the introduction in LBLRTM of P- and R-branch line coupling for CO_2, AERI measurements from the ARM Tropical Western Pacific (TWP) site were used to determine that these previous adjustments were no longer necessary (Payne et al. 2007). More recently, SGP AERI measurements were used along with satellite measurements to modify the CO_2 continuum and line coupling implementation near 2400 cm^{-1} in LBLRTM (Mlawer et al. 2012).

c. Spectral trends

Among the many achievements of the AERI/LBLRTM QME was the establishment of confidence in the accuracy of the AERI radiance observations. Furthermore, since the AERI design allows it to monitor both its calibration and sensitivity every 10 min, it is an ideal sensor for long-term trend analysis, which was one of the original design goals of the multidecadal observations by the ARM Program. Using 14 years of data (1997–2010) collected at the SGP site by the AERI-01 instrument, an analysis was performed to characterize the distribution of the downwelling radiance as a function of clear sky, opaque cloud, and "thin cloud" (Turner and Gero 2011), and then to determine if there were any trends in these classifications over the entire record or when analyzed as a function of season or diurnal cycle. Gero and Turner (2011) identified numerous statistically significant trends in the downwelling radiance over the 14-yr period (e.g., Fig. 14-1, bottom). The trends in the spectrally resolved AERI observations, such as that shown for the autumn in the top panel of Fig. 14-1, allowed these trends to be attributed to trends in PWV (in clear-sky scenes) or in cloud properties (in cloudy scenes).

3. Radiative transfer model development

It is clear from the previous section that the ARM Program has been instrumental in establishing LBLRTM as a state-of-the-science radiative transfer model. This benefits both the ARM scientific community and the larger community as well. LBLRTM is used to train forward models utilized in operational satellite retrievals (Clough et al. 2006; Clerbaux et al. 2007) and data assimilation schemes, to develop radiation codes for climate applications (Mlawer et al. 1997), and to provide reference calculations for model intercomparison studies (Barker et al. 2003; Oreopoulos et al. 2012). The breadth and importance of these applications attests to the value of ARM spectral observations and related research in advancing atmospheric and climate science.

Figure 14-2 shows the spectral improvements made in the longwave radiative transfer model over a period corresponding to ARM's first 20 years for moist (middle panel) and dry (bottom panel) conditions. ARM-related advances are responsible for a large fraction of this improvement. As can be seen in Fig. 14-3, which illustrates the impact on vertical flux of improvements to LBLRTM implemented between 1999 and 2009, significant enhancement in model quality continued into ARM's second decade (Delamere et al. 2010). These model improvements have reduced the overall residuals to a level such that elevated levels of trace gases can be observed (Fig. 14-4; Shephard et al. 2003) and more accurate satellite-based retrievals of temperature and species abundances can be attained (Alvarado et al. 2013). Further discussion of ARM accomplishments related to radiative fluxes can be found in McFarlane et al. (2016, chapter 20).

Although not every application in the infrared requires that scattering be included, the lack of scattering in the radiative transfer solution in LBLRTM posed a problem for conditions in which scattering is an important consideration. For example, the scattering contribution from a single-layer liquid water cloud in the downwelling radiance observed by the AERI can be as large as 12% of the total signal, depending on the liquid water path and the wavelength of the radiation (Turner and Löhnert 2014). This limitation prompted ARM-funded development of two codes that utilize gaseous optical depths from LBLRTM and scattering properties of the medium (e.g., liquid or ice clouds, aerosol layers) to perform scattering calculations at high spectral resolution. The Code for High-resolution Accelerated Radiative Transfer and Scattering (CHARTS; Moncet and Clough 1997) multiple-scattering model uses the adding/doubling technique to perform computationally efficient calculations in plane-parallel atmospheres. For accuracies appropriate for remote sensing applications (e.g., ~0.1% in radiances throughout the thermal region), the computational gain achieved in the radiance calculations may be as high as 3000 compared to other existing multiple scattering algorithms. Among its applications, CHARTS was applied to the modeling of observations from the ground-based AERI interferometer in

Brought to you by NOAA Central Library | Unauthenticated | Downloaded 07/19/23 03:21 PM UTC

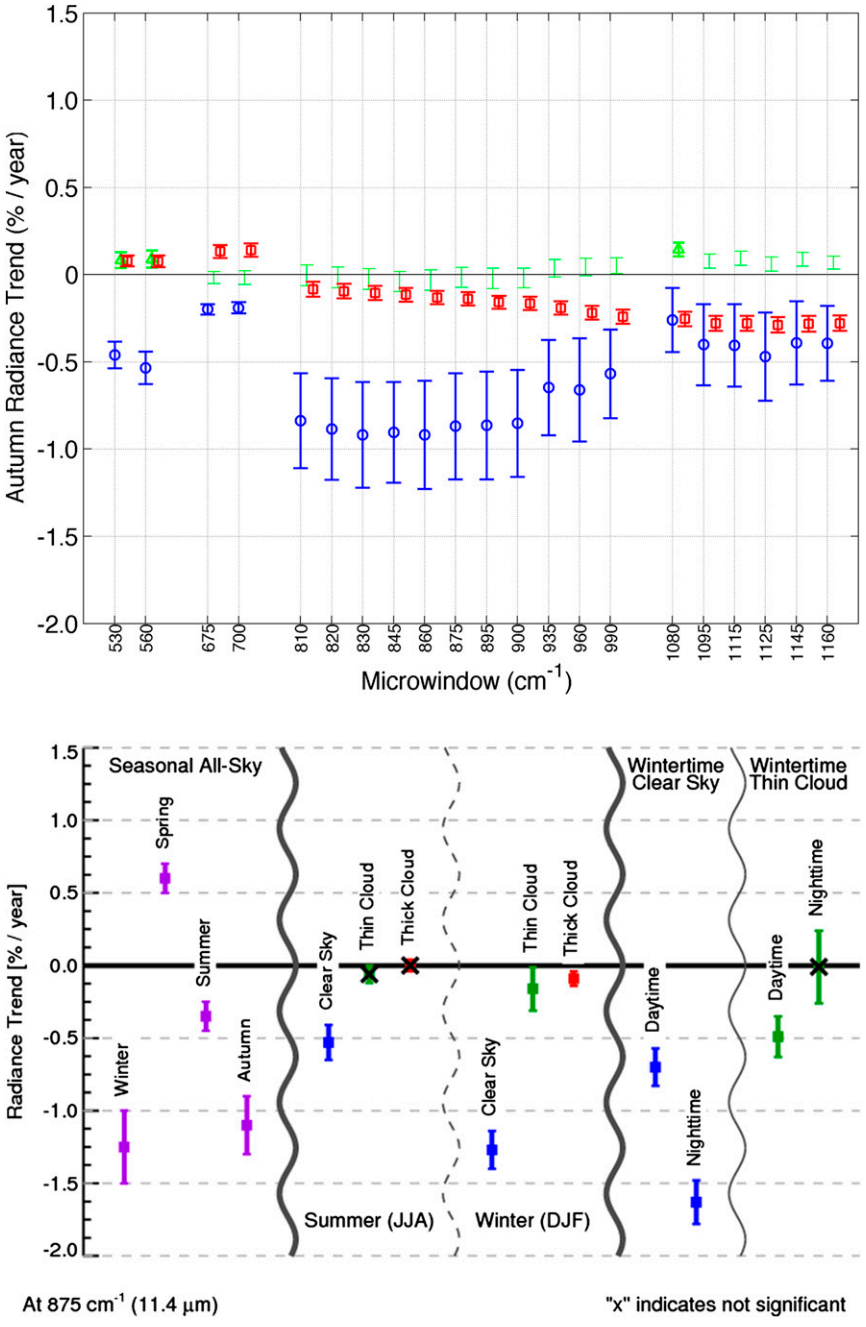

FIG. 14-1. (top) The downwelling spectral radiance trends (% yr^{-1}) for clear sky (blue), opaque clouds (red), and "thin clouds" (green) for the autumn (SON) at the SGP [Fig. 7d from Gero and Turner (2011)]. (bottom) A subset of the trends at 875 cm^{-1} from Gero and Turner (2011) that highlights some of the more interesting findings.

cloudy-sky conditions, used for reference calculations in shortwave radiation code intercomparison studies (e.g., Barker et al. 2003; Oreopoulos et al. 2012), and used for shortwave radiative closure studies (see below).

Another model developed was LBLDIS (Turner et al. 2003), which is a combination of LBLRTM and the Discrete Ordinate Radiative Transfer (DISORT) algorithm (Stamnes et al. 1988). LBLDIS is a flexible model, and is able to compute radiance and flux across a spectrum or in specified spectral intervals (such as a selection of microwindows between absorption lines). This model is the backbone for the

Brought to you by NOAA Central Library | Unauthenticated | Downloaded 07/19/23 03:21 PM UTC

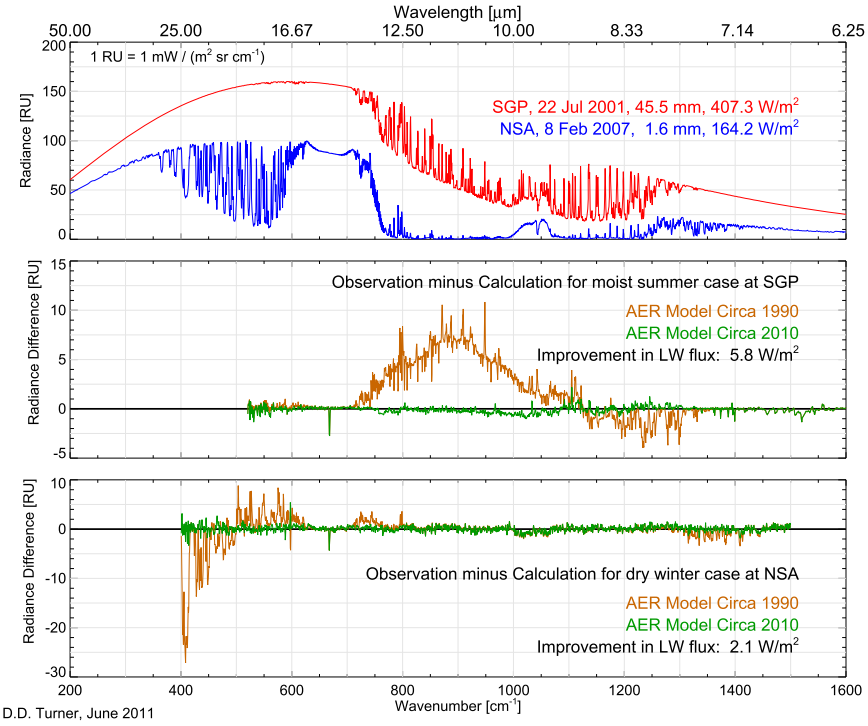

FIG. 14-2. (top) Downwelling infrared radiance computed by LBLRTM for two different cases: a warm, wet case observed at the SGP site (red) and a cold, dry case observed at the NSA site (blue). (middle) The AERI-observed minus LBLRTM-calculated radiance residuals for the warm, wet SGP case, where the LBLRTM calculation was performed using the version of the model that was available at the start of the program in 1990 (brown) and using the version of the model available in 2010 (green). (bottom) As in (middle), but for the cold, dry case using the extended range AERI observations at the NSA site. Note that the improvement in the downwelling longwave (LW) flux includes cancelation of error.

Mixed-Phase Cloud Retrieval Algorithm (MIXCRA; Turner 2005), which is able to retrieve liquid water and ice water optical depths and effective radii of both liquid water and ice particles simultaneously from AERI-observed radiance spectra. Figure 14-5 presents the application of LBLDIS to an AERI observation under extremely dusty conditions observed when the AMF was deployed to Niamey, Niger (Miller and Slingo 2007; Turner 2008). Using an external mixture of kaolinite and hematite spheres, the left panel indicates that good agreement was found between the LBLDIS calculation and the AERI observed radiance in the 600–1400 cm^{-1} region, with the inclusion of scattering in the calculation of radiation making a small, but noticeable, difference. The poor agreement in the 2000–3000 cm^{-1} region most likely reflects inaccurate specification of the aerosol scattering phase function, although the importance of including scattering in the line-by-line calculation is clearly seen.

ARM also contributed to the development of the Santa Barbara DISORT Atmospheric Radiative Transfer (SBDART) program (Ricchiazzi et al. 1998), an easy-to-use moderate resolution code designed for general (including scattering) radiative transfer problems in remote sensing and radiation studies. Although SBDART did not have high enough spectral resolution to compare with individual spectral elements of instruments like the AERI, its convenience for broadband studies or ones involving some amount of spectral resolution made it very popular among researchers. For example, Dufresne et al. (2002) used SBDART to compute the spectral dependence of the radiative forcing, including the effects of scattering, due to mineral aerosols.

4. Clear-sky shortwave studies

The focus of the IRF during the early years of the program was on spectral radiative closure studies in the longwave, a spectral region in which the main absorption sources had clear spectral signatures and the program possessed a well-calibrated radiometric

Brought to you by NOAA Central Library | Unauthenticated | Downloaded 07/19/23 03:21 PM UTC

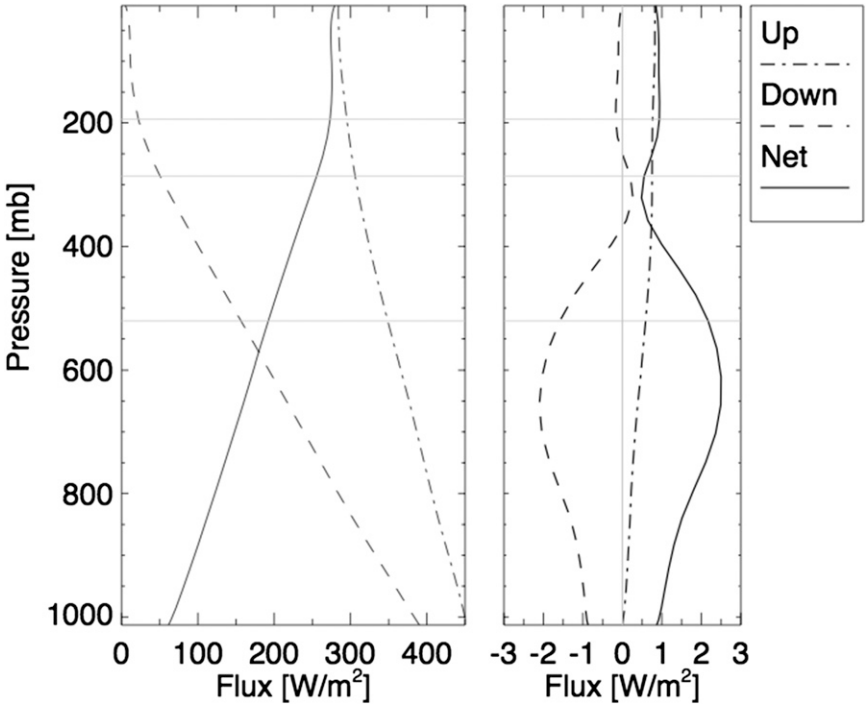

FIG. 14-3. Impact of revisions to LBLRTM on clear-sky longwave fluxes (10–2000 cm^{-1}) for a standard tropical atmosphere. (left) Downwelling, upwelling, and net (up minus down) fluxes computed using LBLRTM from 2009. (right) Differences in computed fluxes (LBLRTM circa 1999 minus LBLRTM from 2009) due to model upgrades.

instrument. Interest and activity in the shortwave region was stimulated after the publication of the broadband radiative closure study of Kato et al. (1997). This study found that, for several clear-sky cases, the modeled shortwave surface downwelling radiation was ~5% greater than the surface irradiance measured by broadband radiometers. This discrepancy also was shown to be mostly in the diffuse component of the shortwave irradiance. This study's analysis of measurement and modeling uncertainties eliminated many possible causes of this lack of agreement, leading the authors to speculate that absorption was due to an unknown "gas X" that may be missing in the model. Subsequent broadband closure studies (e.g., Halthore et al. 1997; Halthore and Schwartz 2000) also demonstrated similar lack of agreement. Given that gaseous absorption occurs primarily in bands consisting of evident absorption lines, this issue was well suited to be addressed through the comparison of spectral shortwave measurements with line-by-line radiative transfer calculations. Although ARM did not possess a single well-calibrated instrument that measured spectrally resolved radiation throughout the entire spectral region in which the majority of solar irradiance occurs, the IRF, under the leadership of Warren Wiscombe and Tony Clough, helped resolve this issue by analyzing measurements from multiple spectral instruments.

Early in the program, support was provided to the University of Denver for development of two instruments to measure spectrally resolved solar radiation, the Absolute Solar Transmittance Interferometer (ASTI; Hawat et al. 2002) and the Solar Radiance Transmission Interferometer (SORTI), the latter of which was configured to provide spectra from 4000 to 13 000 cm^{-1} (750 nm to 2400 nm) with 0.035 cm^{-1} resolution. Unfortunately, the SORTI suffered from a variety of technical issues and was not used heavily by ARM scientists. The ASTI, which measures the direct-solar beam (central 16% of the solar disk) over the spectral range 2000 to 10 000 cm^{-1} with a resolution of 0.6 cm^{-1} (HWHM), was deployed at SGP for an extended period in the 1990s. The instrument was calibrated with a reference tungsten lamp that had a maximum temperature of 2800 K through the same optical path traveled by the solar radiation; this provided the ASTI with an absolute calibration uncertainty of better than 5%. The analysis of the near-infrared spectra from this instrument established that LBLRTM was missing a number of collision-induced oxygen absorption bands, and a parameterization of these bands was developed for the

Brought to you by NOAA Central Library | Unauthenticated | Downloaded 07/19/23 03:21 PM UTC

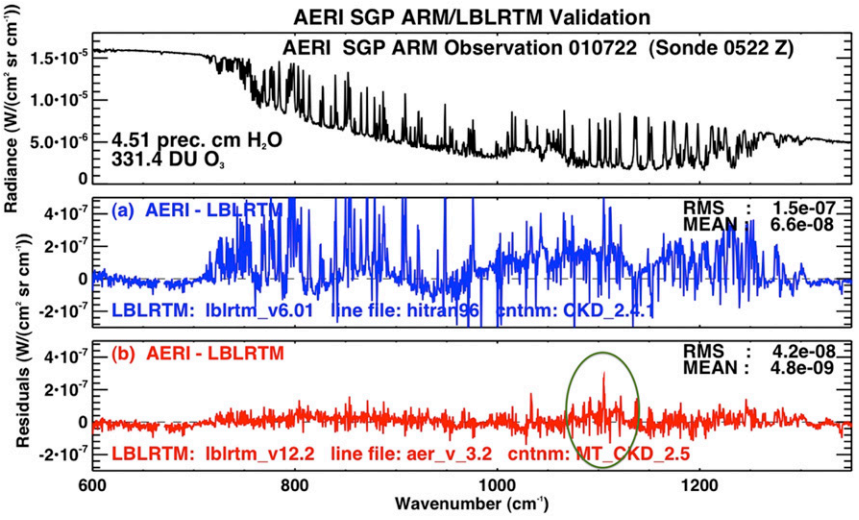

FIG. 14-4. (top) AERI radiance observation from SGP on 22 Jul 2001 for a case with 4.5 cm of PWV; (middle) radiance differences between AERI and LBLRTM calculation using older spectroscopy (HITRAN 96, CKD_2.4.1). (bottom) Radiance differences between AERI and LBLRTM with recent spectroscopic updates (line file - aer_v3.2, MT_CKD_2.5). A spectral feature (the green circle in the bottom panel) associated with formic acid (HCOOH) is identified in the residuals, and is consistent with an atmospheric abundance of this gas equal to ~9 times its assumed background concentration. [This is an updated version of a figure appearing in Shephard et al. (2003).]

CKD continuum model (Mlawer et al. 1998). These absorption bands, which account for less than 1 W m^{-2} of direct-beam absorption for a solar zenith angle of 60°, were the only large residual features observed in the analysis of ASTI spectra (Brown et al. 1998). Figure 14-6 shows a ~2000 cm^{-1} portion of an ASTI observation and the corresponding ASTI-LBLRTM residuals, which indicates overall good agreement despite certain identifiable issues. [See Mlawer et al. (1998) for residuals in this region before and after the inclusion of the collision-induced oxygen bands.] It must be noted that comparisons such as these are not able to uncover spectroscopic errors within saturated bands, nor are they able to detect issues related to very broad absorbers due to the piecewise linear scaling that has been performed on the ASTI spectra to remove the impact of aerosols and instrument calibration error. For all the ASTI cases analyzed, however, there was very good agreement between measurement and calculations for significantly different solar zenith angles and PWV amounts.

Analysis of clear-sky absorption in the remainder of the near-infrared region and the entire visible spectral region was made possible by the deployment at SGP of the Rotating Shadowband Spectroradiometer (RSS; Harrison et al. 1999), developed at the State University of New York at Albany. The RSS detector is either a silicon-diode array or a charge-coupled device (CCD) that is tilted to correct for chromatic aberration and bring all of the dispersed wavelengths at the detector surface to a focus. The out-of-band rejection of stray light is about 10^5, which is considerably better than that of a single grating spectrometer. The RSS uses the shadowband technique to simultaneously measure diffuse and total (and thereby direct) irradiance from 9500 to 28 000 cm^{-1} (360–1050 nm) and can be calibrated with high accuracy using Langley regression in cloud-free and horizontally homogeneous scenes. Even though this instrument's resolution was too coarse to resolve individual absorption lines, analysis of RSS spectra was able to eliminate the possibility of significant unmodeled absorption in the spectral regions observed.

Radiative closure analysis using an early version of the RSS instrument, measuring in 512 channels with spectral resolution ranging from 91 cm^{-1} in the near-IR to 65 cm^{-1} in the ultraviolet, demonstrated that good agreement with LBLRTM/CHARTS calculations could be attained for both direct and diffuse irradiances across the entire spectrum (Mlawer et al. 2001). A sensitivity analysis indicated that the technique used would have detected a source of molecular absorption of the magnitude of the Chappuis band of ozone had it been unknown, which is responsible for less absorbed solar irradiance than the missing absorption that had been speculated in earlier broadband studies. Figure 14-7 presents a case from the extension of this analysis to the 1024-channel RSS. Good overall agreement

Brought to you by NOAA Central Library | Unauthenticated | Downloaded 07/19/23 03:21 PM UTC

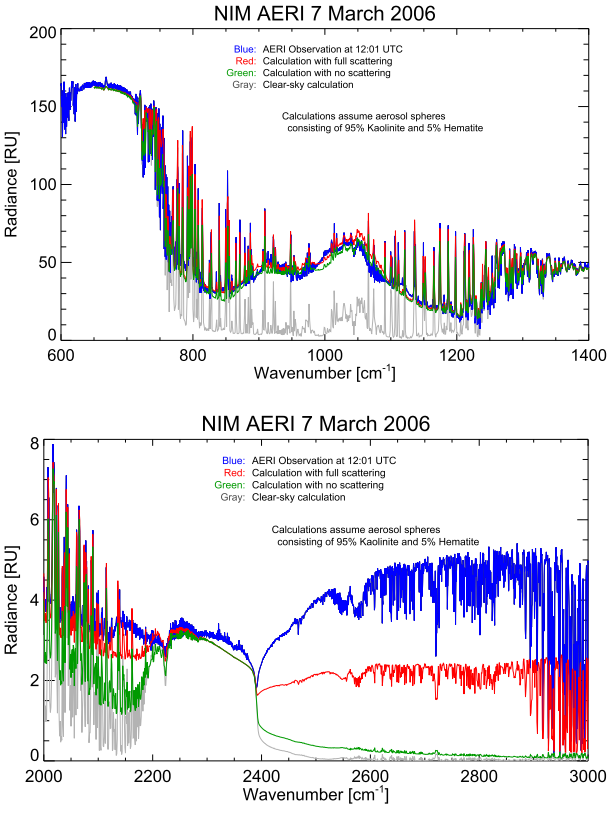

FIG. 14-5. Downwelling radiance observed by the AERI (blue) and computed with the LBLDIS with scattering (red) and without scattering (green) during a dust storm at Niamey for two spectral regions (top: 600–1400 cm^{-1}; bottom: 2000–3000 cm^{-1}) observed by the AERI, where the downwelling radiance in the larger wavenumbers (shorter wavelengths) includes a substantial amount of scattered solar radiation. The calculation assumed that the dust composition was an external mixture of kaolinite and hematite spheres. The gray lines indicate the downwelling radiance that would be observed if there were no dust aerosols in the sky (i.e., a pristine-sky LBLDIS calculation). 1 radiance unit (RU) is 1 mW $(m^2\ sr\ cm^{-1})^{-1}$.

between the measurement and calculation is seen, although direct irradiance residuals associated with the water vapor band at 10 600 cm^{-1} and the oxygen A-band (13 000 cm^{-1}) can be observed. The diffuse residuals in the near-IR are thought to be due to deviation of the aerosol optical depth from the assumed Angstrom relation and/or possible spectral dependence of the aerosol single-scattering albedo.

Through these closure studies with the ASTI and RSS, members of the IRF demonstrated that spectrally resolved measurements and calculations were in basic agreement and there were no unknown absorption bands in the shortwave. Other studies determined that the primary cause of the lack of closure in the broadband studies was flawed radiometric calibration of the instruments (Haeffelin et al. 2001; Dutton et al. 2001). After this issue was corrected, later broadband closure studies (Mlawer et al. 2003; Michalsky et al. 2006), also benefitting from improved model inputs with respect to aerosol and surface properties, demonstrated solid measurement-calculation agreement. [See McFarlane et al. (2016, chapter 20) for further discussion.]

In addition to radiative closure studies, clear-sky RSS measurements have been utilized for numerous applications. Michalsky et al. (1999) used Langley analysis to obtain optical depths from RSS observations, identified six collision-induced oxygen absorption bands in the optical depth spectra, and found no unidentified absorption bands. Kiedron et al. (2001) used RSS measurements in the 10 500 cm^{-1} (940 nm) water vapor band to perform PWV retrievals in dry and cold conditions, and found good correlation with PWV values retrieved from a collocated microwave radiometer. Gianelli et al. (2005) determined from RSS measurements that aerosol size distributions at SGP were bimodal and developed a retrieval to derive information about both the fine and coarse modes, as well as column amounts of NO_2. [Further discussion about the accomplishments in the program with respect to the determination of aerosol properties can be found in McComiskey and Ferrare (2016), chapter 21.] A long-term dataset of extraterrestrial solar irradiance obtained from Langley analysis of RSS spectra was used by Harrison et al. (2003) to analyze and identify issues with commonly used specifications of solar spectral irradiance.

Analyses of measurements of diffuse solar radiation motivated the development of an approach to specify the spectral surface albedo in the vicinity of the SGP site (McFarlane et al. 2011). First, measurements from each channel of two downlooking Multifilter Radiometers (MFRs) at the SGP site (mounted on the 10- and 25-m towers) are used with the corresponding measurement of total irradiance from the uplooking Multifilter Rotating Shadowband Radiometer (MFRSR) to obtain surface albedo values in the five MFR/MFRSR channels. Based upon observed spectral surface reflectances in the Bowker et al. (1985) atlas, the surface albedo values are used to identify a surface type under each tower as snow-covered, green vegetation, nonvegetated (e.g., soil), or partial vegetation, which is a linear combination of green and nonvegetated surfaces given by a Normalized Difference Vegetation Index (NDVI) obtained from the surface albedo values in two of the channels. Based on the same atlas of spectral surface reflectances, the surface albedo values are then used with the identified surface type to obtain a piecewise linear surface albedo function covering the

Brought to you by NOAA Central Library | Unauthenticated | Downloaded 07/19/23 03:21 PM UTC

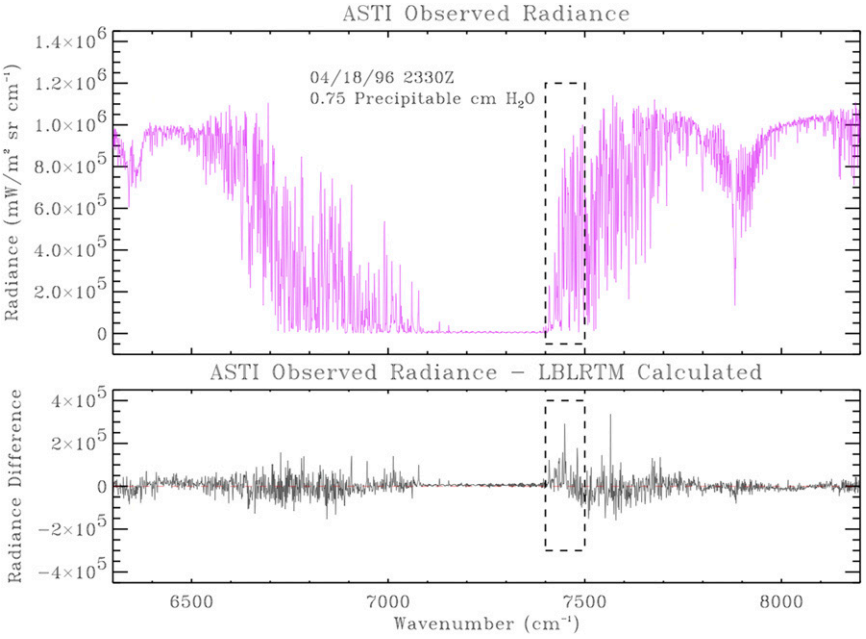

FIG. 14-6. From Brown et al. (1998), (top) ASTI radiance spectra for 6300–8200 cm^{-1} measured on 18 Apr 1996 at SGP for a low PWV case at a solar zenith angle of 71.5°. Notable absorption features seen in this panel are a saturated water vapor band centered at 7200 cm^{-1} and a collision-induced oxygen band at 7800 cm^{-1}. (bottom) Spectral differences between this ASTI observation and a corresponding LBLRTM calculation. Dotted rectangle indicates a region in which the spectral residuals indicated issues with line intensities and widths.

entire shortwave region. Validations of these spectral albedo functions with respect to a spectroradiometer (Trishchenko et al. 2003) showed good agreement for all surface types for wavelengths less than 1280 nm and extending farther into the near-IR for green and nonvegetated surfaces, although a fair amount of variability was seen throughout the near-IR for all surface types. Radiative transfer calculations at SGP typically employ an equal weighting of the spectral surface albedo functions associated with the two MFRs [available as a Value Added Product (VAP) at the ARM Data Archive].

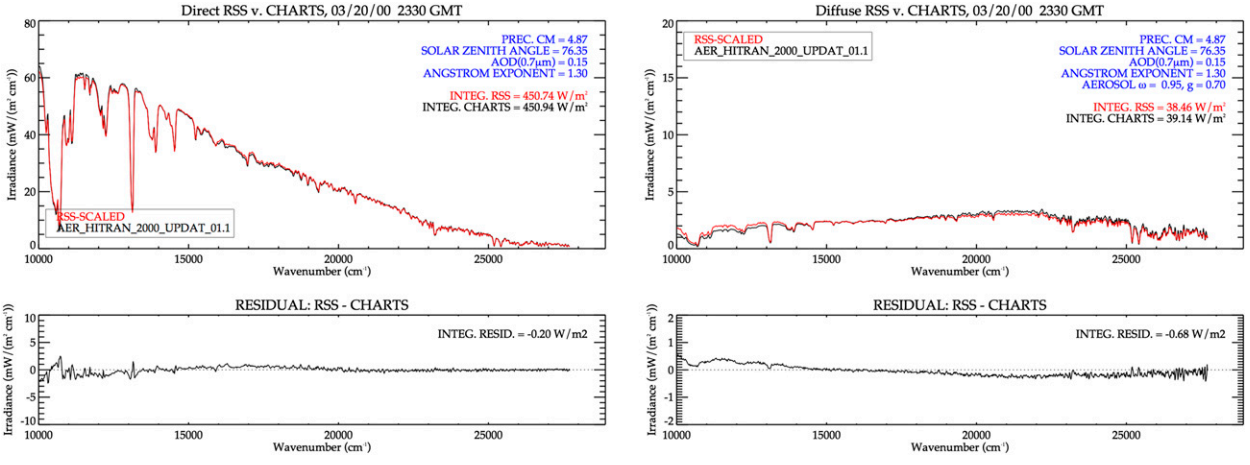

FIG. 14-7. (left top) RSS measurement (red) and LBLRTM/CHARTS calculation (black) of direct irradiance [mW $(m^2\,cm^{-1})^{-1}$] for a clear-sky case on 20 Mar 2000 at SGP. (left bottom) Direct irradiance differences between measurement and calculation. (right top) RSS measurement and LBLRTM/CHARTS calculation of diffuse irradiance for this case. (right bottom) Measurement–calculation differences for diffuse irradiance. Various specifics of the calculations are listed on the plots.

Brought to you by NOAA Central Library | Unauthenticated | Downloaded 07/19/23 03:21 PM UTC

Even with the productive applications of ASTI and RSS measurements, the ARM Radiative Processes Working Group (RPWG; formerly the IRF) identified as a high priority the deployment of a spectral shortwave instrument with greater spectral coverage than both the ASTI and RSS. This led to the development of the Shortwave Spectrometer (SWS), which provides zenith radiance measurements from 4600 to 28 500 cm^{-1} (350–2170 nm). The SWS was deployed alongside the RSS at SGP in the mid-2000s, and a shortwave (SW) QME was established to evaluate these instruments, along with other inputs needed for the SW closure exercise (e.g., the spectral surface albedo product from above and aerosol properties). While radiative closure analysis of a large number of RSS cases with LBLRTM/CHARTS indicated agreement similar to that shown in Fig. 14-7, there were sizeable differences between the SWS measurements and calculations that could not be explained by any reasonable deficiency in either the model or the data used as input to the model (Delamere et al. 2009). Subsequently, field tests determined that the SWS measurement of zenith radiance is susceptible to contamination from direct solar irradiance incident on the instrument fore-optics (i.e., a light leak existed in the instrument). The SWS fore-optics were subsequently redesigned by the instrument mentor team and the instrument was redeployed (Flynn et al. 2010). Evaluation of measurements from the modified SWS is ongoing.

5. Cloudy-sky spectral analyses

Although ARM spectral measurements have not been exploited as extensively for cloudy-sky applications as they have for clear-sky studies, there have been several notable uses of AERI and RSS spectra to further our understanding of cloud optical and microphysical properties.

One advantage of having spectral infrared radiance observations, such as from the AERI, is that they are very sensitive to changes in cloud properties as long as the cloud is not optically thick. The AERI is extremely sensitive to liquid water path (LWP) and effective radius (Reff) when the LWP is less than ~60 $g\,m^{-2}$ and provides a markedly better retrieval of LWP than the microwave radiometer for these smaller LWP values (Turner 2007). This advantage is extremely important since a large fraction of liquid-bearing clouds at all climatic locations have LWP less than 100 $g\,m^{-2}$ (Turner et al. 2007a), and the accurate determination of LWP is critical in order to accurately compute the radiative impact of these clouds (Turner et al. 2007b; Sengupta et al. 2003). Furthermore, since liquid water and ice absorb in different spectral regions observed by the AERI, these observations can be used to retrieve properties of mixed-phase clouds. The MIXCRA retrieval described above has been used extensively to study Arctic clouds (Turner 2005), has been validated with direct measurements of liquid and ice cloud optical depths observed by the polarization-sensitive high-spectral-resolution lidar (Turner and Eloranta 2008), and has been used to retrieve the cloud fraction in the AERI's field of view in broken cumulus cases (Turner and Holz 2005).

Figure 14-8 shows an example of the sensitivity of the infrared radiance to cloud properties. The AERI observed downwelling radiance during the deployment of the AMF at Pt. Reyes, California, in 2005 (Miller et al. 2016, chapter 9). MIXCRA was used to retrieve the cloud properties, and for this case determined that the LWP was 42.2 $g\,m^{-2}$ and Reff was 8.2 μm. The sensitivity of the AERI radiance to changes in LWP and Reff is shown in the bottom panel of Fig. 14-8, as well as the impact on the downwelling radiance if scattering was not included in the calculation. When the AERI-retrieved cloud properties were used to compute the downwelling shortwave radiative flux, the results agreed much better with the flux observation from a collocated pyranometer than flux calculations that used the cloud properties derived from the collocated microwave radiometer (Turner 2007).

An extension of radiative closure studies using RSS spectra to liquid clouds concluded that good spectral measurement–model agreement for diffuse irradiance could be attained with a reasonable choice for effective radius for a homogeneous single-layer cloud (Mlawer et al. 2001). This agreement, plus the impossibility of attaining spectral agreement from adding a small amount of cloud absorption in the near-IR, provided evidence that liquid clouds did not have unknown absorption in the near-IR, as had been speculated (e.g., Valero et al. 1997). The difficulty in finding sufficiently homogeneous clouds limited the applicability of this type of analysis, in which a single set of cloud properties accurately represents the entire cloud in the hemispheric field of view of the RSS. A more sophisticated application of RSS spectra for the study of clouds was established in a series of papers by Min and collaborators that explored the information contained in RSS measurements in the oxygen A-band concerning photon path length and scattering (Harrison and Min 1997; Min and Harrison 1999; Min et al. 2001). This work was later extended to develop a detection method for multilayer clouds (Li and Min 2010), an approach to retrieve vertical profiles of liquid water content, optical depth, and effective size (Li and Min 2013), and motivated the development of the High-Resolution Oxygen A-Band

Brought to you by NOAA Central Library | Unauthenticated | Downloaded 07/19/23 03:21 PM UTC

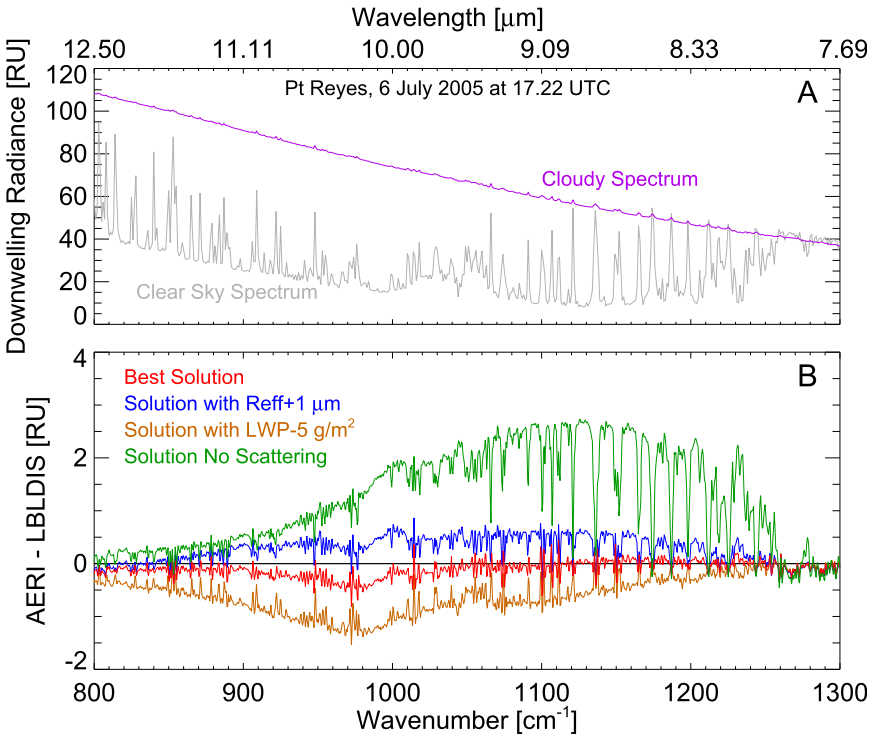

FIG. 14-8. (a) Downwelling radiance (purple) observed by the AERI at Pt. Reyes, California, on 6 Jul 2005, with a simulated clear-sky spectrum (gray). (b) The observed minus computed radiance where the ''best solution'' (red) used the retrieved cloud properties from the MIXCRA algorithm (LWP of 42.2 g m^{-2} and Reff of 8.2 μm). The blue and brown traces show the residuals that would result if the Reff was increased by 1 μm or the LWP was decreased by 5 g m^{-2}, respectively. The green trace shows the residual that would result if the calculation that used the best solution did not include scattering.

Spectrometer (HABS) at the University of Albany (Min et al. 2011).

Other ARM-related spectral instruments also have led to notable results. For example, spectra from a spectroradiometer measuring from 4500 to 28 600 cm^{-1} (350–2200 nm, from Analytical Spectral Devices) that was deployed at NSA in spring 2008 as part of the Indirect and Semi-Direct Aerosol Campaign (ISDAC) were used to study single-layer liquid and mixed-phased clouds. Irradiance measurements in different spectral regions allowed determination of cloud phase and optical depth, and the impact on surface shortwave irradiance of the presence of ice along with liquid in a cloud of fixed optical depth was determined to be typically 5 W m^{-2}, although it could be as great as 8–10 W m^{-2} (Lubin and Vogelmann 2011). Also, in a series of papers and conference presentations (e.g., Marshak et al. 2009; Chiu et al. 2009), measurements from the SWS at SGP were used to explore an intriguing linear relationship exhibited by zenith radiances measured in the transition zone between cloudy and clear regions. This relationship allows a straightforward determination of the optical depth and effective size of liquid clouds (McBride et al. 2013).

6. Summary and looking ahead

The scientific advances that have resulted from analysis of ARM spectral radiometric measurements have been impressive and wide-ranging. Still, several unresolved topics remain for which a spectral perspective will be beneficial, and the program is well positioned to contribute to further progress. As discussed above, the far-IR spectral region had been relatively underexplored, and ongoing analysis of spectral radiance measurements from the ARM RHUBC-I and -II field campaigns should provide a conclusive resolution. There has been preliminary discussion of a third RHUBC campaign, with a focus on cloud-radiative processes in the radiatively potent far-IR region.

The near-IR spectral region also has not received a great deal of attention in the program despite its significant amount of solar radiation, mix of gaseous absorption bands and uncertain amount of water vapor

Brought to you by NOAA Central Library | Unauthenticated | Downloaded 07/19/23 03:21 PM UTC

continuum absorption, and possible utility for constraining aerosol properties and size distributions, as well as cloud property retrievals. The design issues that were uncovered with respect to the SWS (see above) set back potential progress in this area, but occurred at a fortuitous time since funding from the American Recovery and Reinvestment Act (ARRA) of 2009 enabled a significant upgrade of ARM spectral radiometric instrumentation measuring in the near-IR shortly thereafter. The reconfigured SWS, which measures zenith radiance from 4650 to 28 500 cm^{-1} (350–2150 nm) at moderate spectral resolution, was redeployed to SGP in 2011. ARRA also allowed the addition of four Shortwave Array Spectrometers (SAS) to ARM's suite of instruments. The SAS measures from 5900 to 29 400 cm^{-1} at moderate resolution. One version of the SAS measures zenith (SAS-Ze) radiance, while a second version measures hemispheric irradiance (SAS-He); both types have been deployed for a period of time at SGP and during various AMF campaigns. Although the effort to calibrate the SAS has not yet been completed, Lubin et al. (2013) has exploited the spectral content of the SAS-Ze to retrieve cloud phase, optical depth, and effective size for single-phase clouds. Measurements from the SWS and SAS are expected to be valuable in validating ice optical property parameterizations, a topic of notable complexity that has not been the subject of comprehensive radiative closure analysis.

There have been significant recent advances in specifying the spectral optical properties of ice clouds, such as the modified anomalous diffraction approximation (MADA) of Mitchell et al. (1996) and subsequent publications and an approach that combines geometric optics and the finite difference time domain technique (Yang et al. 2000, 2005). The suite of ARM collocated zenith-pointing instruments that span much of the solar and thermal spectrum (SAS, SWS, AERI) will provide information that will be key to their evaluation.

The accomplishments of the ARM Program with respect to the analysis of spectral radiation measurements have fulfilled the aspirations of the ICRCCM participants and the objectives of the program's founders. ARM radiative closure studies have greatly improved our knowledge of the absorption properties of atmospheric constituents and significantly lowered the uncertainties associated with clear-sky radiative transfer, thereby establishing a confident foundation on which to build fast radiative transfer codes for use in atmospheric prediction models. The ARM Program contributed greatly in this area, as detailed in Mlawer et al. (2016, chapter 15). Spectrally resolved radiation measurements at the ARM sites, when coupled with observations from the program's suite of collocated instruments that measure thermodynamic, aerosol, and cloud properties, have also precipitated substantial advances in our understanding of atmospheric processes. These accomplishments, which are due to the efforts of many ARM scientists and infrastructure members, have perhaps even exceeded the ICRCCM recommendations and the original goals of ARM. In the future, ARM spectral measurements are likely to lead to further advances in our knowledge, and add to the program's catalog of spectral successes.

Acknowledgments. The authors would like to acknowledge the leadership of the ARM Instantaneous Radiative Flux (IRF) Working Group and the Water Vapor Intensive Observation Period (WVIOP)—Tony Clough, Bob Ellingson, Hank Revercomb, and Warren Wiscombe—for all their contributions to the work described in this section. Their efforts were essential to the success of spectral radiation research in the ARM Program.

REFERENCES

Alvarado, M. J., V. H. Payne, E. J. Mlawer, G. Uymin, M. W. Shephard, K. E. Cady-Pereira, J. Delamere, and J. Moncet, 2013: Performance of the line-by-line radiative transfer model (LBLRTM) for temperature, water vapor, and trace gas retrievals: Recent updates evaluated with IASI case studies. *Atmos. Chem. Phys.*, **13**, 6687–6711, doi:10.5194/acp-13-6687-2013.

Barker, H. W., and Coauthors, 2003: Assessing 1D atmospheric solar radiative transfer models: Interpretation and handling of unresolved clouds. *J. Climate*, **16**, 2676–2699, doi:10.1175/1520-0442(2003)016<2676:ADASRT>2.0.CO;2.

Bowker, D. E., R. E. Davis, D. L. Myric, K. Stacy, and W. T. Jones, 1985: Spectral reflectances of natural targets for use in remote sensing. NASA Ref. Publ. 1139, 181 pp. [Available online at ntrs.nasa.gov/archive/nasa/casi.ntrs.nasa.gov/19850022138.pdf.]

Brown, P. D., S. A. Clough, E. J. Mlawer, T. R. Shippert, and F. J. Murcray, 1998: High resolution validation in the shortwave: ASTI/LBLRTM QME. *Proc. Eighth ARM Science Team Meeting*, Richland, WA, U.S. Department of Energy, 101–108.

Chiu, C. J., A. Marshak, Y. Knyazikhin, P. Pilewskie, and W. J. Wiscombe, 2009: Physical interpretation of the spectral radiative signature in the transition zone between cloud-free and cloudy regions. *Atmos. Chem. Phys.*, **9**, 1419–1430, doi:10.5194/acp-9-1419-2009.

Cimini, D., F. Nasir, E. R. Westwater, V. H. Payne, D. D. Turner, E. J. Mlawer, M. L. Exner, and M. Cadeddu, 2009: Comparison of ground-based millimeter-wave observations in the Arctic winter. *IEEE Trans. Geosci. Remote Sens.*, **47**, 3098–3106, doi:10.1109/TGRS.2009.2020743.

Clerbaux, C., and Coauthors, 2007: The IASI/MetOp Mission: First observations and highlights of its potential contribution to GMES. *Space Res. Today*, **168**, 19–24, doi:10.1016/S0045-8732(07)80046-5.

Clough, S. A., F. X. Kneizys, and R. W. Davies, 1989: Line shape and the water vapor continuum. *Atmos. Res.*, **23**, 229–241, doi:10.1016/0169-8095(89)90020-3.

——, M. J. Iacono, and J.-L. Moncet, 1992: Line-by-line calculation of atmospheric fluxes and cooling rates: Application to water vapor. *J. Geophys. Res.*, **97**, 15 761–15 785, doi:10.1029/92JD01419.

Brought to you by NOAA Central Library | Unauthenticated | Downloaded 07/19/23 03:21 PM UTC

——, M. W. Shephard, E. J. Mlawer, J. S. Delamere, M. J. Iacono, K. Cady-Pereira, S. Boukabara, and P. D. Brown, 2005: Atmospheric radiative transfer modeling: A summary of the AER codes. *J. Quant. Spectrosc. Radiat. Transfer*, **91**, 233–244, doi:10.1016/j.jqsrt.2004.05.058.

——, and Coauthors, 2006: Forward model and Jacobians for tropospheric emission spectrometer retrievals. *IEEE Trans. Geosci. Remote Sens.*, **44**, 1308–1323, doi:10.1109/TGRS.2005.860986.

Delamere, J., E. Mlawer, J. Michalsky, P. Kiedron, C. Flynn, and C. Long, 2009: Update on shortwave spectral radiative closure studies at the ACRF SGP site. *Proc. 19th ARM Science Team Meeting*, Louisville, KY, U.S. Department of Energy. [Abstract available online at https://www.arm.gov/publications/proceedings/conf19/display?id=NjIw.]

——, S. A. Clough, V. H. Payne, E. J. Mlawer, D. D. Turner, and R. R. Gamache, 2010: A far-infrared radiative closure study in the Arctic: Application to water vapor. *J. Geophys. Res.*, **115**, D17106, doi:10.1029/2009JD012968.

Dufresne, J.-L., C. Gautier, P. Ricchiazzi, and Y. Fouquart, 2002: Longwave scattering effects of mineral aerosols. *J. Atmos. Sci.*, **59**, 1959–1966, doi:10.1175/1520-0469(2002)059<1959:LSEOMA>2.0.CO;2.

Dutton, E. G., J. J. Michalsky, T. Stoffel, B. W. Forgan, J. Hickey, D. W. Nelson, T. L. Alberta, and I. Reda, 2001: Measurement of broadband diffuse solar irradiance using current commercial instrumentation with a correction for thermal offset errors. *J. Atmos. Oceanic Technol.*, **18**, 297–314, doi:10.1175/1520-0426(2001)018<0297:MOBDSI>2.0.CO;2.

Ellingson, R. G., and Y. Fouquart, 1991: The intercomparison of radiation codes in climate models: An overview. *J. Geophys. Res.*, **96**, 8925–8927, doi:10.1029/90JD01618.

——, and W. J. Wiscombe, 1996: The Spectral Radiance Experiment (SPECTRE): Project description and sample results. *Bull. Amer. Meteor. Soc.*, **77**, 1967–1985, doi:10.1175/1520-0477(1996)077<1967:TSREPD>2.0.CO;2.

——, J. Ellis, and S. Fels, 1991: The intercomparison of radiation codes used in climate models: Long wave results. *J. Geophys. Res.*, **96**, 8929–8953, doi:10.1029/90JD01450.

——, R. D. Cess, and G. L. Potter, 2016: The Atmospheric Radiation Measurement Program: Prelude. *The Atmospheric Radiation Measurement (ARM) Program: The First 20 Years, Meteor. Monogr.*, No. 57, Amer. Meteor. Soc., doi:10.1175/AMSMONOGRAPHS-D-15-0029.1.

Flynn, C., and Coauthors, 2010: New shortwave array spectrometers for the ARM Climate Research Facility. *First Atmospheric System Research (ASR) Science Team Meeting*, Bethesda, MD, U.S. Department of Energy. [Abstract available online at http://asr.science.energy.gov/meetings/stm/posters/view?id=238.]

Gero, P. J., and D. D. Turner, 2011: Long-term trends in downwelling spectral infrared radiance over the U.S. Southern Great Plains. *J. Climate*, **24**, 4831–4843, doi:10.1175/2011JCLI4210.1.

Gianelli, S. M., B. E. Carlson, and A. A. Lacis, 2005: Aerosol retrievals using rotating shadowband spectroradiometer data. *J. Geophys. Res.*, **110**, D05203, doi:10.1029/2004JD005329.

Haeffelin, M., S. Kato, A. M. Smith, C. K. Rutledge, T. P. Charlock, and J. R. Mahan, 2001: Determination of the thermal offset of the Eppley precision spectral pyranometer. *Appl. Optics*, **40**, 472–484, doi:10.1364/AO.40.000472.

Halthore, R. N., and S. E. Schwartz, 2000: Comparison of model-estimated and measured diffuse downward irradiance at surface in cloud-free skies. *J. Geophys. Res.*, **105**, 20 165–20 177, doi:10.1029/2000JD900224.

——, ——, J. J. Michalsky, G. P. Anderson, R. A. Ferrare, B. N. Holben, and H. M. Ten Brink, 1997: Comparison of model estimated and measured direct-normal solar irradiance. *J. Geophys. Res.*, **102** (D25), 29 991–30 002, doi:10.1029/97JD02628.

Han, Y., J. A. Shaw, J. H. Churnside, P. D. Brown, and S. A. Clough, 1997: Infrared spectral radiance measurements in the tropical Pacific atmosphere. *J. Geophys. Res.*, **102** (D4), 4353–4356, doi:10.1029/96JD03717.

Harries, J., and Coauthors, 2008: The far-infrared Earth. *Rev. Geophys.*, **46**, RG4004, doi:10.1029/2007RG000233.

Harrison, L., and Q. Min, 1997: Photon pathlength distributions from O_2 A-band absorption. *IRS'96: Current Problems in Atmospheric Radiation*, W. L. Smith and K. Stamnes, Eds., Deepak Publishing, 594–598.

——, M. Beauharnois, J. Berndt, P. Kiedron, J. Michalsky, and Q. Min, 1999: The rotating shadowband spectroradiometer (RSS) at SGP. *Geophys. Res. Lett.*, **26**, 1715–1718, doi:10.1029/1999GL900328.

——, P. Kiedron, J. Berndt, and J. Schlemmer, 2003: Extraterrestrial solar spectrum 360– 1050 nm from Rotating Shadowband Spectroradiometer measurements at the Southern Great Plains (ARM) site. *J. Geophys. Res.*, **108**, 4424, doi:10.1029/2001JD001311.

Hawat, T., T. Stephen, and F. Murcray, 2002: Absolute solar transmittance interferometer for ground-based measurements. *Appl. Opt.*, **41**, 3582–3589, doi:10.1364/AO.41.003582.

Kato, S., T. P. Ackerman, and E. E. Clothiaux, 1997: Uncertainties in modeled and measured clear-sky surface shortwave irradiances. *J. Geophys. Res.*, **102**, 25 881–25 898, doi:10.1029/97JD01841.

Kiedron, P., and Coauthors, 2001: A robust retrieval of water vapor column in dry Arctic conditions using the rotating shadowband spectroradiometer. *J. Geophys. Res.*, **106**, 24 007–24 016, doi:10.1029/2000JD000130.

Knuteson, R. O., B. Whitney, H. E. Revercomb, and F. A. Best, 1999: The history of the University of Wisconsin Atmospheric Emitted Radiance Interferometer (AERI) prototype during the period April 1994 through July 1995. ARM Tech. Rep. TR-001.1, 43 pp. [Available online at http://www.arm.gov/publications/tech_reports/arm-tr-001.1.pdf.]

——, and Coauthors, 2004a: The Atmospheric Emitted Radiance Interferometer (AERI). Part I: Instrument design. *J. Atmos. Oceanic Technol.*, **21**, 1763–1776, doi:10.1175/JTECH-1662.1.

——, and Coauthors, 2004b: The Atmospheric Emitted Radiance Interferometer (AERI). Part II: Instrument performance. *J. Atmos. Oceanic Technol.*, **21**, 1777–1789, doi:10.1175/JTECH-1663.1.

Kollias, P., and Coauthors, 2016: Development and applications of ARM millimeter-wavelength cloud radars. *The Atmospheric Radiation Measurement (ARM) Program: The First 20 Years, Meteor. Monogr.*, No. 57, Amer. Meteor. Soc., doi:10.1175/AMSMONOGRAPHS-D-15-0037.1.

Li, S., and Q. Min, 2010: Diagnosis of multilayer clouds using photon path length distributions. *J. Geophys. Res.*, **115**, D20202, doi:10.1029/2009JD013774.

——, and ——, 2013: Retrievals of vertical profiles of stratus cloud properties from combined oxygen A-band and radar observations. *J. Geophys. Res. Atmos.*, **118**, 769–778, doi:10.1029/2012JD018282.

Lubin, D., and A. Vogelmann, 2011: The influence of mixed-phase clouds on surface shortwave irradiance during the Arctic spring. *J. Geophys. Res.*, **116**, D00T05, doi:10.1029/2011JD015761.

Brought to you by NOAA Central Library | Unauthenticated | Downloaded 07/19/23 03:21 PM UTC

——, ——, and C. Flynn, 2013: Retrieval of cloud microphysical properties from the new shortwave array spectroradiometer. *Proc. Fourth Atmospheric System Research (ASR) Science Team Meeting*. Potomac, MD, U.S. Department of Energy. [Abstract available online at http://asr.science.energy.gov/meetings/stm/posters/view?id=808.]

Marshak, A., Y. Knyazikhin, J. C. Chiu, and W. J. Wiscombe, 2009: Spectral invariant behavior of zenith radiance around cloud edges observed by ARM SWS. *Geophys. Res. Lett.*, **36**, L16802, doi:10.1029/2009GL039366.

McBride, P., A. Marshak, Y. Knyazkhin, J. Chiu, and W. Wiscombe, 2013: What can be learned from ARM shortwave hyperspectral observations? *Fourth Atmospheric System Research (ASR) Science Team Meeting*. Potomac, MD, U.S. Department of Energy. [Abstract available online at http://asr.science.energy.gov/meetings/stm/posters/view?id=918.]

McComiskey, A., and R. A. Ferrare, 2016: Aerosol physical and optical properties and processes in the ARM Program. *The Atmospheric Radiation Measurement (ARM) Program: The First 20 Years, Meteor. Monogr.*, No. 57, Amer. Meteor. Soc., doi:10.1175/AMSMONOGRAPHS-D-15-0028.1.

McFarlane, S. A., K. L. Gaustad, E. J. Mlawer, C. N. Long, and J. Delamere, 2011: Development of a high spectral resolution surface albedo product for the ARM Southern Great Plains central facility. *Atmos. Meas. Tech.*, **4**, 1713–1733, doi:10.5194/amt-4-1713-2011.

——, J. H. Mather, and E. J. Mlawer, 2016: ARM's progress on improving atmospheric broadband radiative fluxes and heating rates. *The Atmospheric Radiation Measurement (ARM) Program: The First 20 Years, Meteor. Monogr.*, No. 57, Amer. Meteor. Soc., doi:10.1175/AMSMONOGRAPHS-D-15-0046.1.

Michalsky, J. J., M. Beauharnois, J. Berndt, L. Harrison, P. Kiedron, and Q. Min, 1999: O_2-O_2 absorption band identification based on optical depth spectra of the visible and near-infrared. *Geophys. Res. Lett.*, **26**, 1581–1584, doi:10.1029/1999GL900267.

——, and Coauthors, 2006: Shortwave radiative closure studies for clear skies during the Atmospheric Radiation Measurement 2003 Aerosol Intensive Observation Period. *J. Geophys. Res.*, **111**, D14S90, doi:10.1029/2005JD006341.

Miller, M. A., and A. Slingo, 2007: The ARM Mobile Facility and its first international deployment: Measuring radiative flux divergence in West Africa. *Bull. Amer. Meteor. Soc.*, **88**, 1229–1244, doi:10.1175/BAMS-88-8-1229.

——, K. Nitschke, T. P. Ackerman, W. R. Ferrell, N. Hickmon, and M. Ivey, 2016: The ARM Mobile Facilities. *The Atmospheric Radiation Measurement (ARM) Program: The First 20 Years, Meteor. Monogr.*, No. 57, Amer. Meteor. Soc., doi:10.1175/AMSMONOGRAPHS-D-15-0051.1.

Min, Q., and L. C. Harrison, 1999: Joint statistics of photon pathlength and cloud optical depth. *Geophys. Res. Lett.*, **26**, 1425–1428, doi:10.1029/1999GL900246.

——, ——, and E. E. Clothiaux, 2001: Joint statistics of photon pathlength and cloud optical depth: Case studies. *J. Geophys. Res.*, **106**, 7375–7385, doi:10.1029/2000JD900490.

——, B. Yin, J. Berndt, L. Harrison, and P. Kiedron, 2011: A high-resolution oxygen A-band spectrometer (HABS) and photon path length distribution. *Fall AGU Meeting*, San Francisco, CA, Amer. Geophys. Union, Abstract A11H-0200.

Mitchell, D. L., A. Macke, and Y. Liu, 1996: Modeling cirrus clouds. Part II: Treatment of radiative properties. *J. Atmos. Sci.*, **53**, 2967–2988, doi:10.1175/1520-0469(1996)053<2967:MCCPIT>2.0.CO;2.

Mlawer, E. J., S. J. Taubman, P. D. Brown, M. J. Iacono, and S. A. Clough, 1997: Radiative transfer for inhomogeneous atmospheres: RRTM, a validated correlated-k model for the longwave. *J. Geophys. Res.*, **102**, 16 663–16 682, doi:10.1029/97JD00237.

——, S. A. Clough, P. D. Brown, T. M. Stephen, J. C. Landry, A. Goldman, and F. J. Murcray, 1998: Observed atmospheric collision-induced absorption in near-infrared oxygen bands. *J. Geophys. Res.*, **103**, 3859–3863, doi:10.1029/97JD03141.

——, and Coauthors, 2001: Comparisons between RSS measurements and LBLRTM/CHARTS calculations for clear and cloudy conditions. *Proc. 11th ARM Science Team Meeting*, Atlanta, GA, U.S. Department of Energy. [Available online at http://www.arm.gov/publications/proceedings/conf11/extended_abs/mlawer_ej.pdf.]

——, and Coauthors, 2003: Recent developments on the broadband heating rate profile value-added product. *Proc. 13th ARM Science Team Meeting*, Broomfield, CO, U.S. Department of Energy. [Available online at http://www.arm.gov/publications/proceedings/conf13/extended_abs/mlawer-ej.pdf.]

——, V. H. Payne, J.-L. Moncet, J. S. Delamere, M. J. Alvarado, and D. C. Tobin, 2012: Development and recent evaluation of the MT_CKD model of continuum absorption. *Philos. Trans. Roy. Meteor. Soc.*, **370A**, 2520–2556, doi:10.1098/rsta.2011.0295.

——, M. J. Iacono, R. Pincus, H. Barker, L. Oreopoulos, and D. Mitchell, 2016: Contributions of the ARM Program to radiative transfer modeling for climate and weather applications. *The Atmospheric Radiation Measurement (ARM) Program: The First 20 Years, Meteor. Monogr.*, No. 57, Amer. Meteor. Soc., doi:10.1175/AMSMONOGRAPHS-D-15-0041.1.

Moncet, J.-L., and S. A. Clough, 1997: Accelerated monochromatic radiative transfer for scattering atmospheres: Application of a new model to spectral radiance observations. *J. Geophys. Res.*, **102**, 21 853–21 866, doi:10.1029/97JD01551.

Oreopoulos, L., and Coauthors, 2012: The continual intercomparison of radiation codes: Results from Phase I. *J. Geophys. Res.*, **117**, D06118, doi:10.1029/2011JD016821.

Payne, V. H., J.-L. Moncet, and S. A. Clough, 2007: Improved spectroscopy for microwave and infrared satellite data assimilation. *JCSDA Fifth Workshop on Satellite Data Assimilation,* College Park, MD, Joint Center for Satellite Data Assimilation. [Available online at http://www.jcsda.noaa.gov/documents/meetings/wkshp7/Session1_RT_Clouds/payne_jcsda_meeting_may2007.pdf.]

——, E. J. Mlawer, K. E. Cady-Pereira, and J.-L. Moncet, 2011: Water vapor continuum absorption in the microwave. *IEEE Trans. Geosci. Remote Sens.*, **49**, 2194–2208, doi:10.1109/TGRS.2010.2091416.

Revercomb, H. E., and Coauthors, 2003: The ARM Program's water vapor intensive observation periods: Overview, accomplishments, and future challenges. *Bull. Amer. Meteor. Soc.*, **84**, 217–236, doi:10.1175/BAMS-84-2-217.

Ricchiazzi, P., S. Yang, C. Gautier, and D. Sowle, 1998: SBDART: A research and teaching software tool for plane-parallel radiative transfer in the Earth's atmosphere. *Bull. Amer. Meteor. Soc.*, **79**, 2101–2114, doi:10.1175/1520-0477(1998)079<2101:SARATS>2.0.CO;2.

Rothman, L. S., 1992: The HITRAN atmospheric molecular spectroscopic database. *Proc. Second ARM Science Team Meeting*, Washington, D.C., U.S. Department of Energy, 15–20.

Brought to you by NOAA Central Library | Unauthenticated | Downloaded 07/19/23 03:21 PM UTC

Sengupta, M., E. E. Clothiaux, T. P. Ackerman, S. Kato, and Q. Min, 2003: Importance of accurate liquid water path for estimation of solar radiation in warm boundary layer clouds: An observational study. *J. Climate*, **16**, 2997–3009, doi:10.1175/1520-0442(2003)016<2997:IOALWP>2.0.CO;2.

Shephard, M. W., A. Goldman, S. A. Clough, and E. J. Mlawer, 2003: Spectroscopic improvements providing evidence of formic acid in AERI-LBLRTM validation spectra. *J. Quant. Spectrosc. Radiat. Transfer*, **82**, 383–390, doi:10.1016/S0022-4073(03)00164-X.

Shupe, M. D., J. M. Comstock, D. D. Turner, and G. G. Mace, 2016: Cloud property retrievals in the ARM Program. *The Atmospheric Radiation Measurement (ARM) Program: The First 20 Years, Meteor. Monogr.*, No. 57, Amer. Meteor. Soc., doi:10.1175/AMSMONOGRAPHS-D-15-0030.1.

Stamnes, K., S. C. Tsay, W. J. Wiscombe, and K. Jayaweera, 1988: A numerically stable algorithm for discrete-ordinate-method radiative transfer in multiple scattering and emitting layered media. *Appl. Opt.*, **27**, 2502–2509, doi:10.1364/AO.27.002502.

Stokes, G. E., and S. E. Schwartz, 1994: The Atmospheric Radiation Measurement (ARM) Program: Programmatic background and design of the cloud and radiation test bed. *Bull. Amer. Meteor. Soc.*, **75**, 1201–122, doi:10.1175/1520-0477(1994)075<1201:TARMPP>2.0.CO;2.

Strow, L. L., S. E. Hannon, S. De-Souza Machado, H. E. Mottler, and D. C. Tobin, 2006: Validation of the atmospheric infrared sounder radiative transfer algorithm. *J. Geophys. Res.*, **111**, D09S06, doi:10.1029/2005JD006146.

Tobin, D. C., and Coauthors, 1999: Downwelling spectral radiance observation at the SHEBA ice station: Water vapor continuum measurements from 17 to 26 μm. *J. Geophys. Res.*, **104**, 2081–2092, doi:10.1029/1998JD200057.

Trishchenko, A. P., Y. Luo, M. Cribb, Z. Li, and K. Hamm, 2003: Surface spectral albedo intensive operational period at the ARM SGP site in August 2002: Results, analysis, and future plans. *Proc. 13th ARM Program Science Team Meeting*, Richland, WA, U.S. Department of Energy. [Available online at http://www.arm.gov/publications/proceedings/conf13/extended_abs/trishchenko-ap.pdf.]

Turner, D. D., 2005: Arctic mixed-phase cloud properties from AERI lidar observations: Algorithm and results from SHEBA. *J. Appl. Meteor.*, **44**, 427–444, doi:10.1175/JAM2208.1.

——, 2007: Improved ground-based liquid water path retrievals using a combined infrared and microwave approach. *J. Geophys. Res.*, **112**, D15204, doi:10.1029/2007JD008530.

——, 2008: Ground-based infrared retrievals of optical depth, effective radius, and composition of airborne mineral dust above the Sahel. *J. Geophys. Res.*, **113**, D00E03, doi:10.1029/2008JD010054.

——, and R. E. Holz, 2005: Retrieving cloud fraction in the field-of-view of a high-spectral-resolution infrared radiometer. *IEEE Geosci. Remote Sens. Lett.*, **2**, 287–291, doi:10.1109/LGRS.2005.850533.

——, and E. W. Eloranta, 2008: Validating mixed-phase cloud optical depth retrieved from infrared observations with high spectral resolution lidar. *IEEE Geosci. Remote Sens. Lett.*, **5**, 285–288, doi:10.1109/LGRS.2008.915940.

——, and E. J. Mlawer, 2010: The Radiative Heating in Underexplored Bands Campaigns (RHUBC). *Bull. Amer. Meteor. Soc.*, **91**, 911–923, doi:10.1175/2010BAMS2904.1.

——, and P. J. Gero, 2011: Downwelling 10 μm radiance temperature climatology for the Atmospheric Radiation Measurement Southern Great Plains site. *J. Geophys. Res.*, **116**, D08212, doi:10.1029/2010JD015135.

——, and U. Löhnert, 2014: Information content and uncertainties in thermodynamic profiles and liquid cloud properties retrieved from the ground-based Atmospheric Emitted Radiance Interferometer (AERI). *J. Appl. Meteor. Climatol.*, **53**, 752–771, doi:10.1175/JAMC-D-13-0126.1.

——, S. A. Ackerman, B. A. Baum, H. E. Revercomb, and P. Yang, 2003: Cloud phase determination using ground-based AERI observations at SHEBA. *J. Appl. Meteor.*, **42**, 701–715, doi:10.1175/1520-0450(2003)042<0701:CPDUGA>2.0.CO;2.

——, and Coauthors, 2004: The QME AERI LBLRTM: A closure experiment for downwelling high spectral resolution infrared radiance. *J. Atmos. Sci.*, **61**, 2657–2675, doi:10.1175/JAS3300.1.

——, S. A. Clough, J. C. Liljegren, E. E. Clothiaux, K. Cady-Pereira, and K. L. Gaustad, 2007a: Retrieving liquid water path and precipitable water vapor from Atmospheric Radiation Measurement (ARM) microwave radiometers. *IEEE Trans. Geosci. Remote Sens.*, **45**, 3680–3690, doi:10.1109/TGRS.2007.903703.

——, and Coauthors, 2007b: Thin liquid water clouds: Their importance and our challenge. *Bull. Amer. Meteor. Soc.*, **88**, 177–190, doi:10.1175/BAMS-88-2-177.

——, U. Loehnert, M. Cadeddu, S. Crewell, and A. Vogelmann, 2009: Modifications to the water vapor continuum in the microwave suggested by ground-based 150 GHz observations. *IEEE Trans. Geosci. Remote Sens.*, **47**, 3326–3337, doi:10.1109/TGRS.2009.2022262.

——, A. Merrelli, D. Vimont, and E. J. Mlawer, 2012a: Impact of modifying the longwave water vapor continuum absorption model on community Earth system model simulations. *J. Geophys. Res.*, **117**, D04106, doi:10.1029/2011JD016440.

——, and Coauthors, 2012b: Ground-based high spectral resolution observations of the entire terrestrial spectrum under extremely dry conditions. *Geophys. Res. Lett.*, **39**, L10801, doi:10.1029/2012GL051542.

——, E. J. Mlawer, and H. E. Revercomb, 2016: Water vapor observations in the ARM Program. *The Atmospheric Radiation Measurement (ARM) Program: The First 20 Years, Meteor. Monogr.*, No. 57, Amer. Meteor. Soc., doi:10.1175/AMSMONOGRAPHS-D-15-0025.1.

Uttal, T., and Coauthors, 2002: Surface heat budget of the Arctic Ocean. *Bull. Amer. Meteor. Soc.*, **83**, 255–275, doi:10.1175/1520-0477(2002)083<0255:SHBOTA>2.3.CO;2.

Valero, F. P. J., R. D. Cess, M. Zhang, S. K. Pope, A. Bucholtz, B. Bush, and J. Vitko Jr., 1997: Absorption of solar radiation by the cloudy atmosphere: Interpretations of collocated aircraft measurements. *J. Geophys. Res.*, **102** (D25), 29 917–29 927, doi:10.1029/97JD01782.

Varanasi, P., 1998: Laboratory spectroscopy in support of the Atmospheric Radiation Measurement program. *Proc. Seventh ARM Science Team Meeting,* Washington, D.C., U.S. Department of Energy, 277.

Yang, P., K. N. Liou, K. Wyser, and D. Mitchell, 2000: Parameterization of the scattering and absorption properties of individual ice crystals. *J. Geophys. Res.*, **105**, 4699–4718, doi:10.1029/1999JD900755.

——, H. Wei, H.-L. Huang, B. A. Baum, Y. X. Hu, G. W. Kattawar, M. I. Mishchenko, and Q. Fu, 2005: Scattering and absorption property database for nonspherical ice particles in the near through far-infrared spectral region. *Appl. Opt.*, **44**, 5512–5523, doi:10.1364/AO.44.005512.

Brought to you by NOAA Central Library | Unauthenticated | Downloaded 07/19/23 03:21 PM UTC